FOSSIL ENERGY

260
6-18-79

DR. 2757
2757

FE-2031-13

MASTER

MASTER

CHEMISTRY AND STRUCTURE OF COAL-DERIVED ASPHALTENES

Phase III

Quarterly Progress Report for July—September 1978

By
T. F. Yen

Work Performed Under Contract No. EX-76-C-01-2031

University of Southern California
Los Angeles, California

U. S. DEPARTMENT OF ENERGY

DISCLAIMER

NOTICE

Available from the National Technical Information Service, U. S. Department of Commerce, Springfield, Virginia 22161.

Price: Paper Copy $5.25
Microfiche $3.00

FE-2031-13
Distribution Category UC-90a

CHEMISTRY AND STRUCTURE OF COAL-DERIVED ASPHALTENES

Phase III

Quarterly Progress Report for the Period
July — September 1978

Senior Research Associate: Irving Schwager
Graduate Students: Man-Kin Chan
Jonathan Kwan
Win-Chung Lee
Kuang-Hua Shu
Victoria Weinberg
Technical Assistants: Jeffery Miller
Lilly Chung
Principle Investigator: T. F. Yen

University of Southern California
Los Angeles, California 90007

PREPARED for the UNITED STATES
DEPARTMENT of ENERGY

Under Contract No. E(49-18)-2031

Abstract

Preparative scale GPC separation of Synthoil asphaltene was carried out on styrene-divinyl benzene packing (Bio-Beads S-X8). The elution took place in the order of high to low molecular weight. Analyses indicate that aromatic ring systems with large saturated substituents elute first followed by more aromatic molecules with less saturated substituents.

Infrared measurements on coal-derived asphaltenes were carried out with a large path cell (1 cm) in order to measure absorbance as a function of concentration in dilute solution down to 0.3 g/l where association between asphaltenes is not significant. Values for a_{OH} afforded a good linear correlation vs. weight percent OH, determined by the silylation method, $a_{OH} = 0.065$ wt. % OH, and a fair correlation between a_{NH}, and weight percent pyrrolic nitrogen obtained from elemental analysis of chromatographically separated or HCl treated asphaltenes which were also subjected to methylation to remove remaining basic nitrogen, $a_{NH} = 0.050$ wt. % Pyrrolic Nitrogen.

VPO molecular weight studies indicate that coal-derived oils and resins undergo very little association in the solvent THF in the range 4 - 30 g/l in contrast to coal-derived asphaltenes and benzene insolubles.

Thermal treatment of a Synthoil Coal liquid solvent fraction (oil + resin), in tetralin (1:2 wt. ratio) at 232°C for 20 hours resulted in the transformation of 3 - 10 % of the oil + resin into asphaltene. These results support the proposed reversibility of coal liquefaction steps:

$$\text{Asphaltene} \rightleftharpoons \text{Oil} + \text{Resin}$$

Pyrolysis of coal-derived asphaltenes has been shown to produce residues that are characteristic of coalesced mesophase. Asphaltenes from three liquefaction processes, Catalytic Incorporated SRC, Synthoil, and FMC-COED, were pyrolyzed under a nitrogen atmosphere at 20°C/hr. to 360°C and at 5°C/hr. to 420°C. Crossed polarized light reflection micrographs showed a coarse deformed structure for Synthoil asphaltene, a coarse, but not deformed structure for Cat. Inc. asphaltene, and fine isotropic structure for FMC-COED asphaltene.

OBJECTIVE AND SCOPE OF WORK

It is the objective of this project to isolate the asphaltene fractions from coal liquids from a number of liquefaction processes. These asphaltene fractions may be further separated by both gradient elution through column chromatography, and molecular size distribution through gel permeation chromatography.

These coal-derived asphaltene fractions will be investigated by various chemical and physical methods for characterization of their structures. After the parameters are obtained, these parameters will be correlated with the refining, and conversion variables which control a given type of liquefaction process. The effects of asphaltene in catalysis, ash or metal removal, desulfurization and denitrification will also be correlated. It is anticipated that understanding the role of asphaltene in liquefaction processes will enable engineers to both improve existing processes, and to make recommendations for operational changes in planned liquefaction units in the United States.

The objective of Phase III is to continue the characterization of coal asphaltenes and other coal liquid fractions by the use of physical, instrumental and chemical methods. The structural parameters will be used to postulate hypothetical average structures for coal liquid fractions.

SUMMARY OF PROGRESS TO DATE

During this quarter the following tasks have been undertaken and/or completed:

(1) Sample separations and interconversions.

(2) Training of new technical personnel is continuing.

(3) Establishment of sample data bank.

(4) Chromatography of asphaltenes is being carried out.

(5-16) Characterization of coal liquid fractions by various physical and instrumental methods is continuing.

(17) Characterizaion of asphaltenes by densimetric methods.

(19) Characterization of asphaltenes by chemical methods is being carried out.

These tasks are listed in the milestone chart in Fig. 1. Detailed Discussion of technical progress is found in the next section.

Detailed Discussion of Technical Progress

(1) Sample Acquisition, Separation, and Interconversion

Work Accomplished:

(a) Solvent Separation of Coal Liquids

Coal liquid samples were solvent fractionated by the standard method in order to obtain stockpiles of the various solvent fractions.

(b) GPC Separation of Asphaltenes

Analytical gel permeation chromatography (GPC) molecular weight studies were previously carried out on coal-derived asphaltenes isolated from the coal liquids of the five demonstration processes under study (1). Weight average molecular weights, determined by the GPC method, were reported. We now wish to report preliminary results obtained by a preparative scale GPC method in which asphaltenes are separated into a limited number of fractions of relatively narrow molecular size ranges. These fractions are weighed, and characterized by VPO molecular weight determination, elemental analyses, and a variety of instrumental methods.

Fig. 1. Milestone Chart

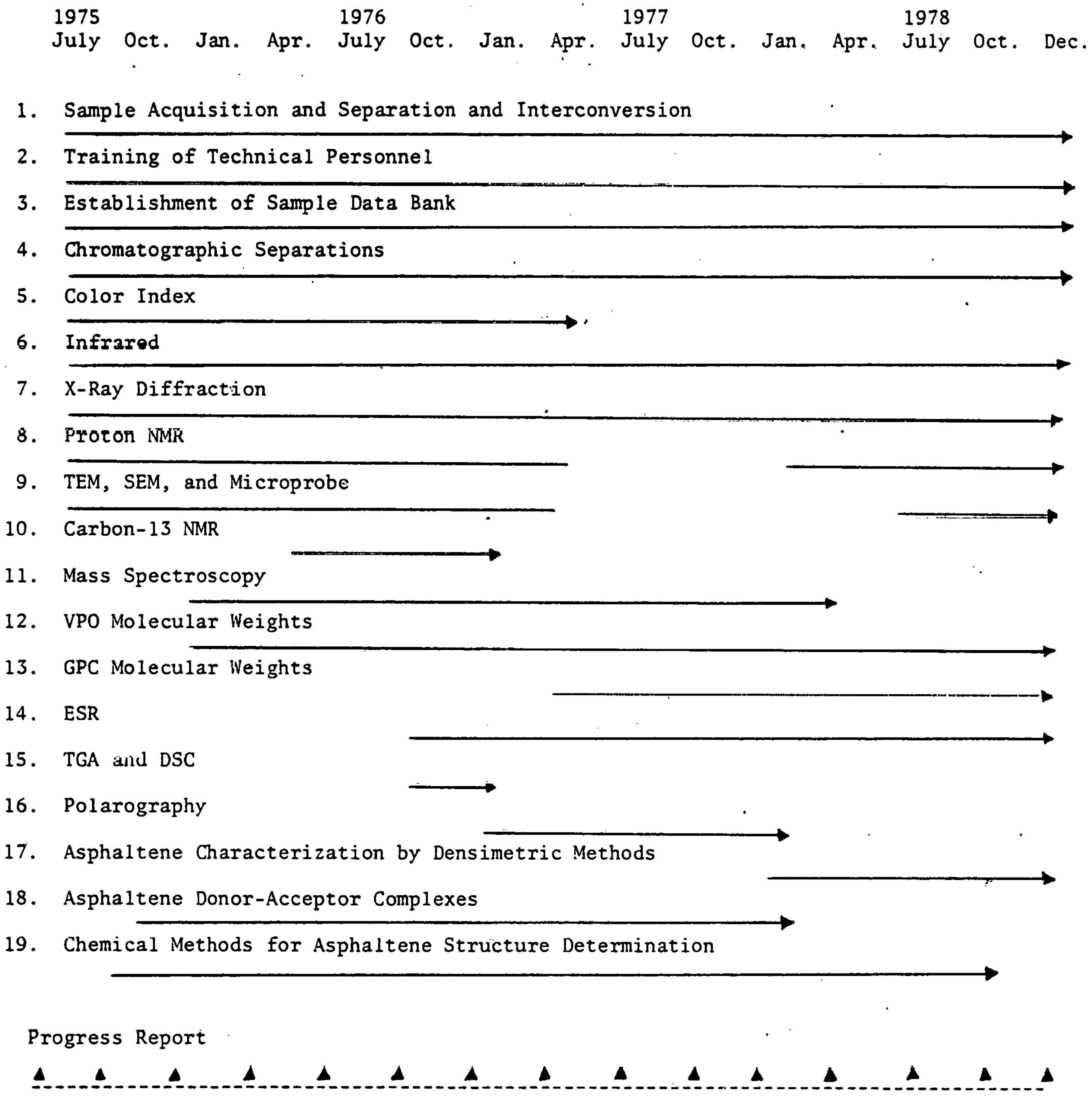

Preparative scale GPC separations were carried out with an Alltech Associates 25 mm ID X 1 m glass column, slurry packed with Bio-Rad, S-X8 , Bio-Beads (200-400 mesh, 8% crosslinked, styrene-divinyl benzene). The column was connected to a Waters Associates HPLC system (2). Tetrahydrofuran (THF) (freshly distilled from sodium) was used as solvent. A typical GPC run is presented Fig. 2 . Generally a three-ml sample, containing ≈1g of asphaltene, was loaded onto the top of the column, and a flow rate of ≈2 ml/min. was used to elute the sample. Pressures of 5 - 10 psig were sufficient to obtain reasonable flow rates. The progress of the chromatograph was generally followed by use of the differential refractive index detector, because UV absorption was too strong except at the beginning and final stages of elution. The fractionated GPC samples were stripped of solvent on a rotary evaporator and freeze dried to powders from benzene. The last trace of benzene was removed by heating the powders overnight in a vacuum oven.

The manufacturer reports Bio-Beads, S-X8 to have a molecular weight exculsion limit of 1,000. We found that a polypropylene oxide standard of MW 2,000 was excluded, whereas a similar standard of MW 800 was not excluded. At the lower molecular weight separation range anthracene could be separated from benzene, but tetralin and toluene could not be separated. In the mid-range aromatics such as 9,10-diphenyl-anthracene could be separated (almost to baseline) from 1,2-benzanthracene on our column. Reinjection of fraction two afforded only a relatively narrow peak indicating that the sample size was sufficiently small to avoid overloading the column.

The weight fraction recovery and VPO molecular weights of the fractions are shown on Fig. 2 . The average molar properties of the fractions, derived from elemental analyses, VPO molecular weight determination and

FIG. 2 GPC CHROMATOGRAM OF SYNTHOIL ASPHALTENE

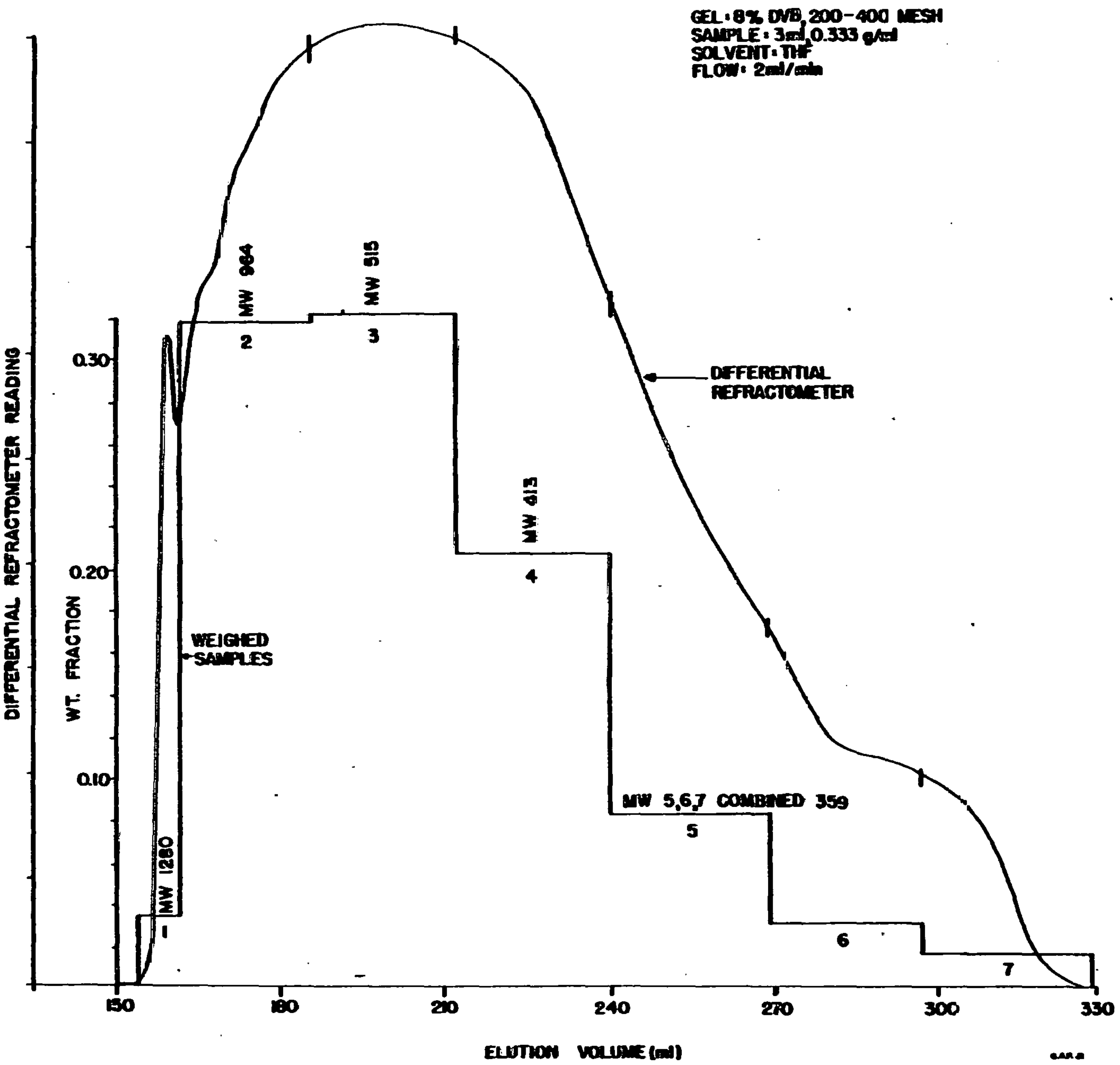

Brown-Ladner NMR analyses, are presented in Table I . The elution took place in the order of high to low molecular weight. The C/H ratio generally increases as the MW decreases, and the % oxygen shows a large decrease in Cut 5. The aromaticity, f_a, shows a steady increase from 0.58 to 0.76 with fraction number, while the number of carbon atoms per saturated substituent, n, decreases from 2.5 to 1.5. The fraction of available aromatic edge atoms occupied by substituents, σ , also decreases from 0.69 to 0.37 as the elution volume increases. These results can be interpreted in terms of aromatic ring systems, with large saturated substituents eluting first. As the elution volume increases the saturated substituents decrease in number and size resulting in the molecules becoming smaller and more aromatic. The size of the average aromatic ring system, as measured by the ratio of substitutable aromatic edge atoms to total aromatic atoms, H_{aru}/C_{ar}, appears to go through a minimum at Cut 3.

Work Forecast:

Additional coal liquid fractions will be separated and characterized by the preparative scale GPC method. X-ray diffraction analysis will be utilized to determine the average layer diameters of GPC fractions.

Table I . Average Molar Properties[a] of Synthoil GPC Fractions[b]

	Cut 1	Cut 2	Cut 3	Cut 4	Cut 5
Molecular Formula	$C_{89.01}H_{84.33}N_{1.96}O_{5.61}S_{0.27}$	$C_{68.00}H_{61.03}N_{1.69}O_{3.51}S_{0.19}$	$C_{35.98}H_{23.78}N_{0.81}O_{2.18}S_{0.08}$	$C_{29.04}H_{25.27}N_{0.68}O_{1.62}S_{0.11}$	$C_{25.96}H_{21.00}N_{0.65}O_{0.75}S_{0.15}$
Molecular Weight	(1280)[c]	964[d]	515[d]	413[d]	359[d]
H_{ar}*	11	25	30	32	42
H_{α}*	35	42	45	46	40
H_{o}*	54	33	25	22	18
f_a	0.58	0.66	0.67	0.70	0.76
H_{aru}/C_{ar}	0.57	0.70	0.83	0.76	0.69
σ	0.69	0.52	0.50	0.48	0.37
R_S	20.5	16.3	9.9	7.5	5.0
n	2.5	1.8	1.5	1.5	1.5
C_A	51.4	45.0	24.1	20.5	19.8
R_a	11.9	7.8	3.1	3.5	4.1
Weight %	3.2	31.6	32.0	20.5	12.7

---

[a] Brown-Ladner Method X=Y=2.

[b] Collected from Bio-Beads SX-8, THF solvent.

[c] VPO THF (Single point).

[d] VPO THF (Extrapolated to infinite dilution).

(c) Solubility Parameters of Coal Liquid Fractions

In our last Quarterly Report (3) we presented preliminary solubility parameter (δ) calculations for Synthoil coal liquid fractions, and for the asphaltenes obtained from the five demonstration processes under study. The calculations were based on the Lawson and Ingham semi-empirical correlation between solubility paramenters and refractive indices (4):

$$\delta \simeq \sqrt{C \, \frac{n^2 - 1}{n^2 + 1}} \qquad (1)$$

where n is refractive index, and C is a constant which depends on the type of compound. An average value of C, obtained from 57 hydrocarbons, 305, was used in equation (1).

We now present extended and improved calculations of solubility parameters. Instead of using the average value of C, (305) in Eq. (1), we calculate weighted values of C which depend on the ratio of aromatic to aliphatic carbons in each coal liquid fraction and the value of C given by Lawson and Ingham for aromatic compounds (287.6) and branched aliphatic hydrocarbons (230.9). The calculated δ values are presented in Table II , and are seen to be in reasonable agreement with experimentally determined δ values. This suggests a convenient method for rapidly estimating δ values of coal-derived products.

Table II Estimated Solubility Parameter, δ_{calc}, For Coal Liquid Products

Solvent Fractions	Synthoil	HRI	CAT. INC.	PAMCO	FMC
	Coal Liquid Process				
Oil	9.0	9.4	10.1	9.3	9.1
Resin	9.6	9.7	10.3	10.6	9.7
Asphaltene	9.8[a]	10.1	10.5	10.5[b]	9.8
Carbene	10.5[a]	10.8	11.2	11.1	10.2
Carboid	10.7[a]	10.8	10.8	11.3[b]	10.4

[a] Experimentally measured maximum solubility range δ values: Asphaltene, 9-12; Carbene, 10-12; Carboid, 10.6-12.

[b] Experimentally measured maximum solubility range δ values: Asphaltene, 8-12; Carboid, 9-12.

(d) Inter-Conversion of Coal Liquid Fractions

An autoclave system equipped with injection loading and withdrawal systems for introducing and removing samples without disturbing the reaction has been constructed this Quarter. Figure 3 is a scheme of the whole system. The temperature controller set has been calibrated. It only shows 1.5% error in temperature reading and 5% deviation in constant temperature control.

A preliminary experiment has been run with a mixture of 2:1 ratio of tetralin to Synthoil pentane soluble fraction. About 40 grams of tetralin were charged to the reaction, and a mixture of 40 grams of tetralin and the Synthoil pentane soluble fraction was charged to the liquid feed vessel. After the temperature of the tetralin in the reactor was raised to 450°F (232°C), the mixture in the liquid feed vessel was forced into the reactor,and the reaction began and lasted for about 20 hours. Samples of 10 ml each were taken afterward without disturbing the reaction and were vacuum-distilled to remove unreacted tetralin. The residue was then separated by the standard solvent separation procedures (5) into three fractions: pentane soluble fraction, asphaltene (pentane insoluble-benzene soluble), and benzene insoluble fractions.

The results of this preliminary experiment shows that 3 to 10% of reactant was converted into asphaltene, while less than 1% of benzene insolubles were formed. It seems that either equilibrium has not been achieved or that the equilibrium lies far toward oil and resin. The former means that the rate of reaction is slow under these conditions. The latter could mean that a large portion of asphaltene would be converted to oil and resin. More experiments should be and will be undertaken in order to study the interconversion and draw any conclusion.

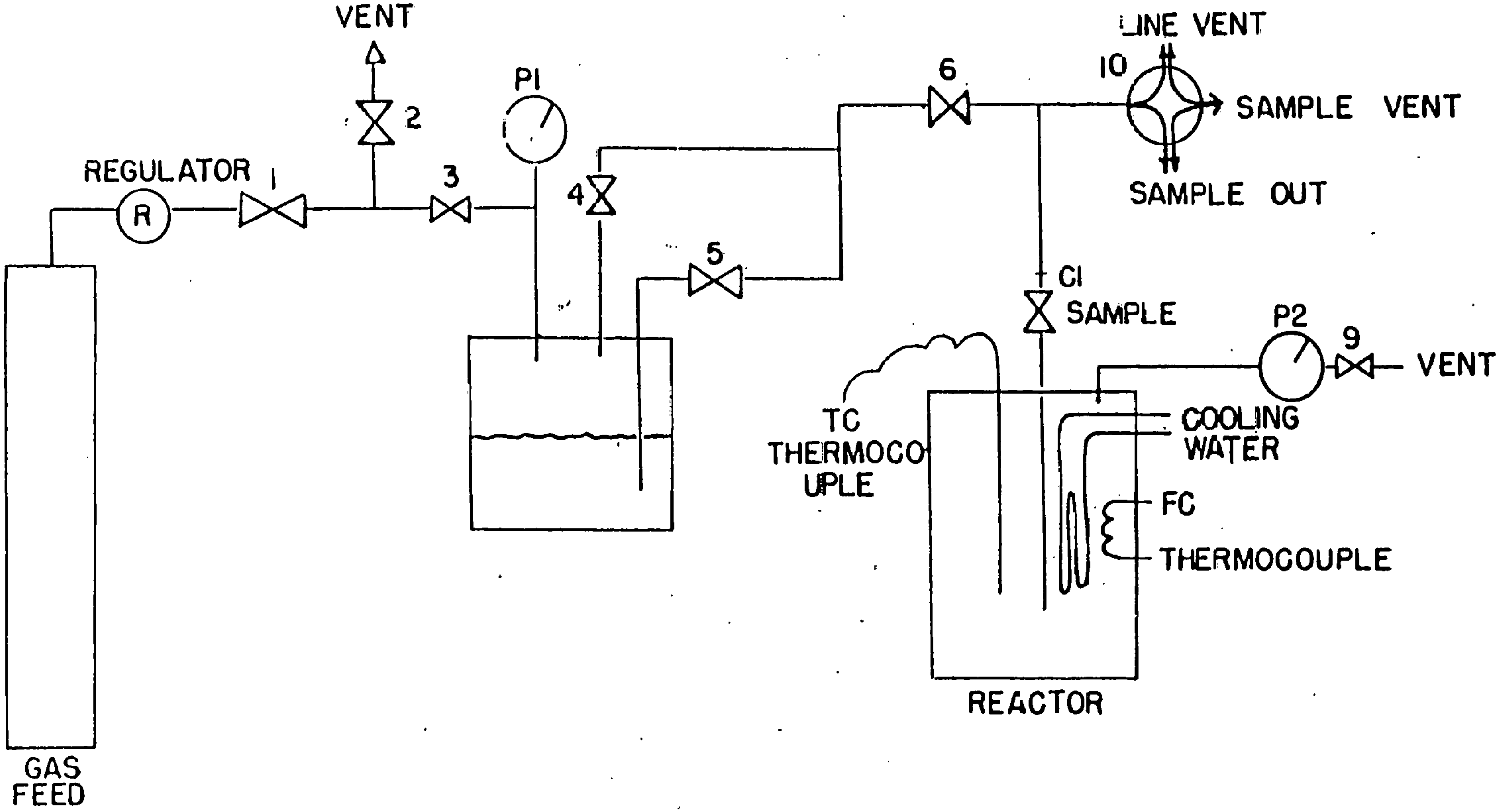

FIG. 3. SAMPLE ENTERING AND REMOVING SYSTEM

(e) Mesophase Formation From Coal Liquid Fractions

In all coal liquefaction processes varying amounts of organic insoluble matter (IOM) are formed. In a pyrolysis process such as the FMC-COED process up to 65% of this coke-like material may be formed (6). In an SRC process such as PAMCO SRC II 6 - 9% of such material is formed (7). Catalyzed hydrogenation processes such as the HRI H-COAL, and the Synthoil process also afford IOM. In addition, these processes suffer from catalyst deactivation due to carbon deposition. A solid residue formed in an SRC plant was found to have anisotropic structures that are characteristic of coalesced mesophase (8). Penn State workers independently produced mesophase from SRC. We have therefore begun to investigate the formation of mesophase from solvent fractionated coal liquid products.

When the organic precursors to coke and synthetic graphite are pyrolyzed, large, flat, polynuclear aromatic molecules are formed by the reactions of aromatic polymerization. As the molecular weight approaches 1500, the molecules condense to form parallel arrays with the structural characteristics of a lamellar liquid crystal. These lamellar liquid crystals are the carbonaceous mesophase. The mesophase transformation usually occurs between 400 °C and 500 °C. Chemical studies indicate that freshly formed mesophase consists of planar aromatic molecules as shown in Figure (4) (9).

In the early stages of nucleation and growth, the mesophase appears as small anisotropic spherules suspended in an optically isotropic matrix. The structure of the spherules consists of aromatic layer molecules that lie perpendicular to the polar diameter

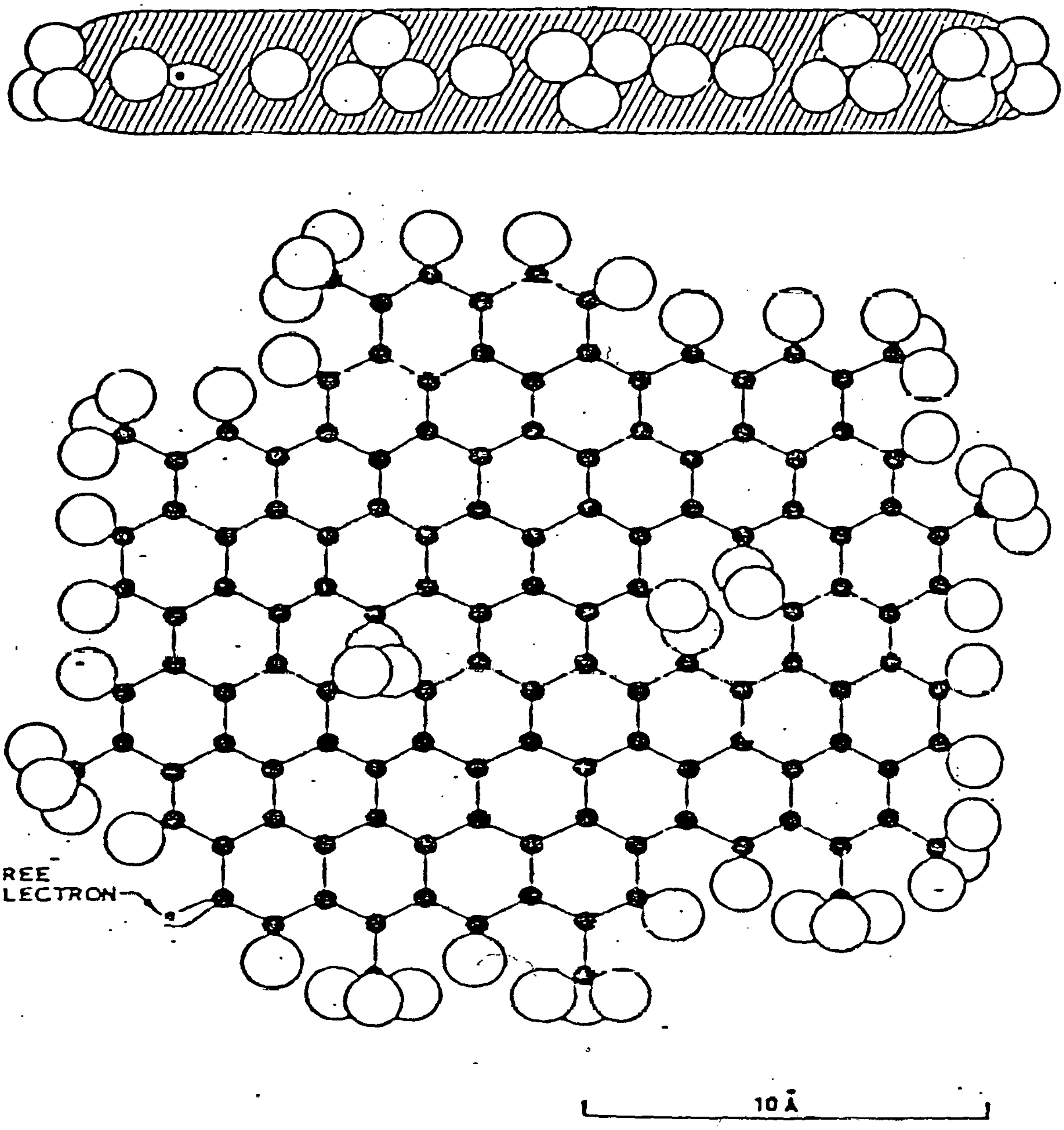

Figure 4 Hypothetical Mesophase Molecule (with a molecular weight near 1600. This model includes dangling methyl groups, vacant sites in the aromatic lattice, and a broken bond (free electron)).

but splay outward to reach the interface with the pyrolyzing matrix normally as shown in Figure (5).

As pyrolysis proceeds, the mesophase spherules grow at the expense of the fluid matrix and sink through it. When the spherules meet, they coalesce to produce larger droplets of more complex structure. This process has been recognized to be the key to the development of graphitizable carbon (10). Materials that go through the mesophase transformation will graphitize and those which do not undergo this transformation will not graphitize.

The formation of the mesophase microstructure follows a systematic pattern which relates primarily to the plasticity of the mesophase and the deformation the plastic mesophase goes through as it hardens into semi coke (11). This effect is shown schematically in Figure (6).

Non-coalescence or fine mosaic isotropic structure results from a fast reacting pyrolyzing mass. The system loses fluidity and the growth of the mesophase is suppresssed. In general, fine mosaic structures result form mesophase which is fully transformed below 430 °C. A flow-type or coalesced anisotropy results when the mesophase retains sufficient plasticity to respond to thermal convection currents and bubble movement. Mesophase which precipitates above 430 °C is extensively deformed to give coarse structures. When the mesophase remains plastic at 455 °C to 465 °C, a fine, fibrous structure or needle coke morphology results. This type of mesophase is preferred for the production of carbon fiber materials.

The size and chemical reactivity of the precursor molecules control the size and viscosity of the units of growth of the anisotropic mesophase, and it is the viscosity of the mesophase, both before and

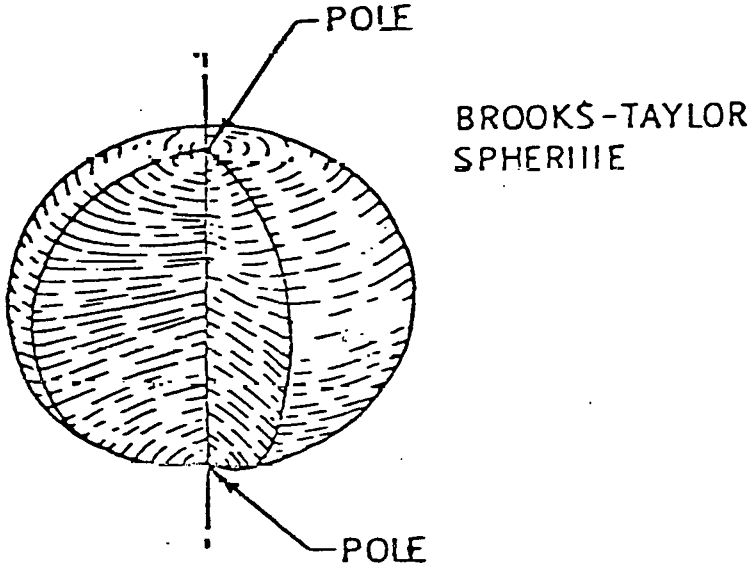

Figure 5 Mesophase Spherule (sectioned on the polar diameter to display the characteristic Brooks-Taylor sphere).

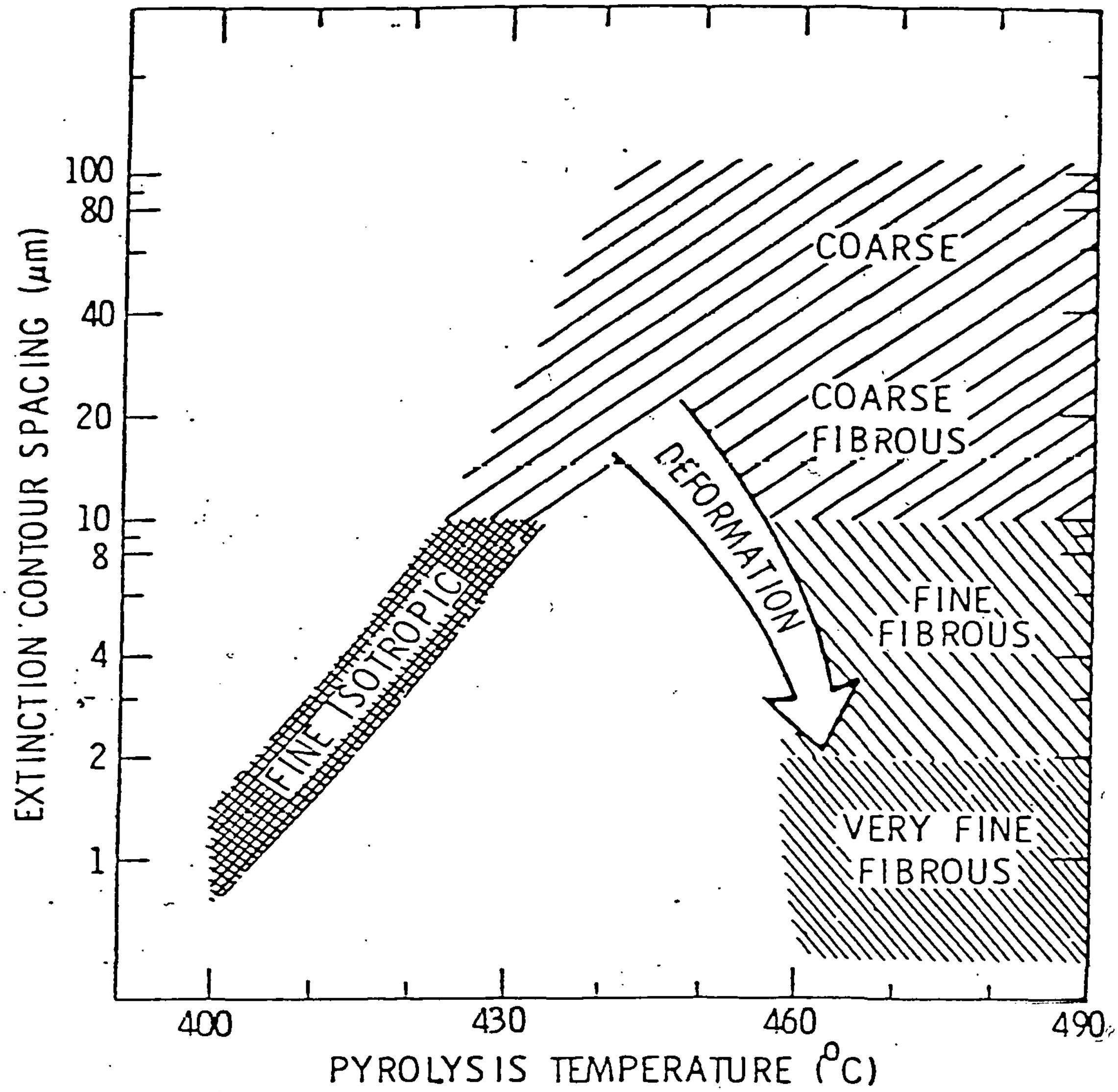

Figure 6 Pattern of Formation of Mesophase Microconstituents of Coke (produced from various precursors by pyrolysis at 5° C/hr, The microstructures are defined in terms of the shape and spacing of the polarized-light extinction contours observed under crossed polarizers).

after coalescence, which determines the character of the final graphite product. The best mesophase is normally formed from planar fused-ring molecules such as naphthalene or anthracene. These materials are usually graphitizable. But if the original molecule is non-planar or if non-planar intermediates are formed as with fluorene or biphenyl, the material will probably not graphitize as well because free rotation inhibits the formation of the ordered planar sheets of the mesophase. Also, phenolic oxygen in the starting material is believed to reduce mesophase growth by inducing cross-linking between molecules.

Asphaltenes from three liquefaction processes, Catalytic Incorporated SRC, Synthoil and FMC-COED, were pyrolyzed under a nitrogen atmosphere to 420 °C. The samples were heated at 20 °C/hr. to 360 °C and at 5 °C/hr to 420 °C. The weight percent residues, after heat treatment, consisted of 66.7%, 66.66% and 51.84% by weight of the starting Catalytic Incorporated, Synthoil, and FMC-COED samples respectively. Crossed polarized light reflection micrographs were obtained for each of the pyrolyzed samples and are shown in Figures 7, 8, and 9. The Catalytic Incorporated asphaltene forms a coarse structure. The Synthoil asphaltene forms a coarse deformed structure and FMC-COED asphaltene forms a fine isotropic structure and is completely transformed at 420 °C. These preliminary results can be related to the oxygen content of the starting material. Table III gives the elemental analysis of the three materials. Phenolic oxygen is believed to cause cross-linking and reduce mesophase plasticity. The Synthoil asphaltene has the lowest phenolic oxygen content, 2.71% and forms a mesophase that remains plastic at 420 °C giving the coarse, deformed structure. The Catalytic Inc. SRC asphaltene contains slightly more phenolic oxygen, 3.38%, and forms a coarse but not a deformed structure. And the

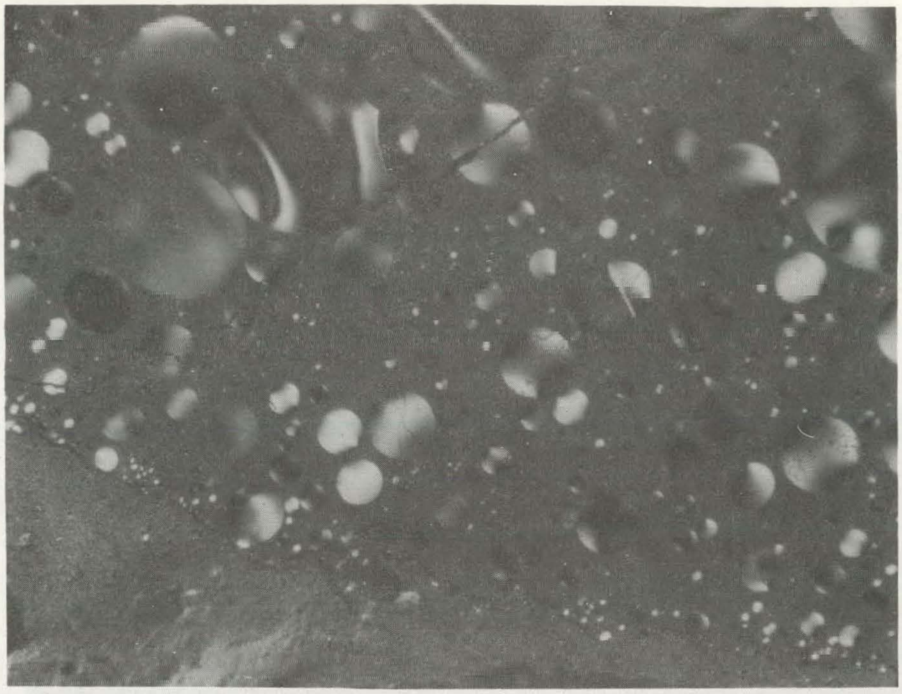

Figure 7. Catalytic Inc. SRC Asphaltene Microstructure
(Crossed Polarizers 200X)

Figure 8. Synthoil Asphaltene Microstructure
(Crossed Polarizers 200X)

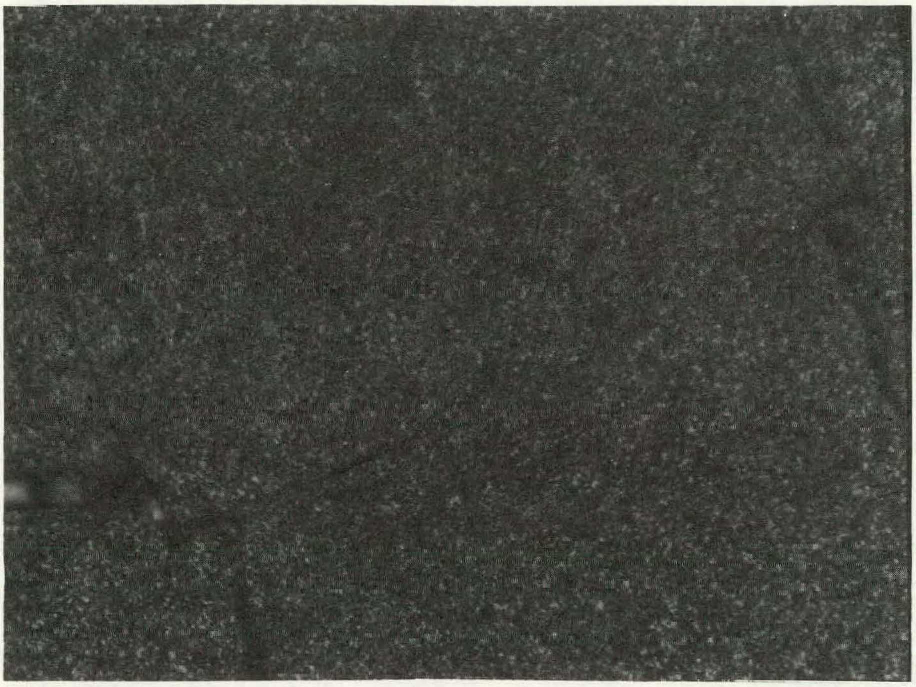

Figure 9. FMC-COED Asphaltene Microstructure (Crossed Polarizers 200X)

FMC-COED contains 5.90% phenolic oxygen and forms the fine isotropic structure which results from crosslinking and solidification at a temperature below 420 °C.

Work Forecast:

Additional coal liquid solvent fractions will be pyrolyzed under controlled conditions to determine their susceptibility toward mesophase formation.

Table III. Elemental Analysis of Coal Liquid Asphaltenes

	Weight %					
	C	H	N	S	O[a]	OH[b]
Catalytic INC. SRC	88.79	5.61	1.25	0.12	4.23	3.38
Synthoil	87.27	6.51	1.63	0.66	3.93	2.71
FMC-COED	82.14	6.47	1.70	2.58	7.11	5.90

[a] By Difference.

[b] Determined by NMR analysis for silylated asphaltene.

(2) Characterization of Coal Liquids by Physical Methods

Work Accomplished:

(a) Infrared

Because of the simplicity of infrared spectroscopic methods for analyzing the concentrations of OH and NH in coal liquid fractions, we have developed procedures for determining the absorptivity of these groups. Previously we reviewed the assignments of the various peaks in the OH and NH regions (3200-3600 cm^{-1}) (3). Preliminary correlations between weight precent OH and NH, and the absorbances of the monomeric OH and NH infrared stretching bands at 3600 and 3470 cm^{-1} were presented in the last Quarterly Report (3). During the present Quarter we obtained a cell with a large enough path (1 cm) to measure absorbance as a function of concentration in dilute solution down to 0.3 g/l where association between asphaltenes is not significant. Plots of absorbance vs. concentrations were generally linear below concentrations of 10 g/l and could be extrapolated to a value of zero at infinite dilution (Figs. 10,11). However, some of the asphaltenes (FMC-COED, Cat. Inc. SRC) afforded deviations from linearity at concentrations approaching 5 g/l. Such deviations support the general premise that asphaltene association via hydrogen bonding (12,13), and concomitant loss of monomeric OH absorption are related. The extrapolated slopes of the linear portion of such plots were used to obtain absorptivity values (Table IV). These values for a_{OH} afforded a good linear correlation vs. weight percent OH, determined by the silylation method (14) (Fig. 12), and a fair correlation

FIG. 10 CORRELATION OF SYNTHOIL ASPHALTENE NH ABSORBANCE VS CONCENTRATION IN $CDCl_3$

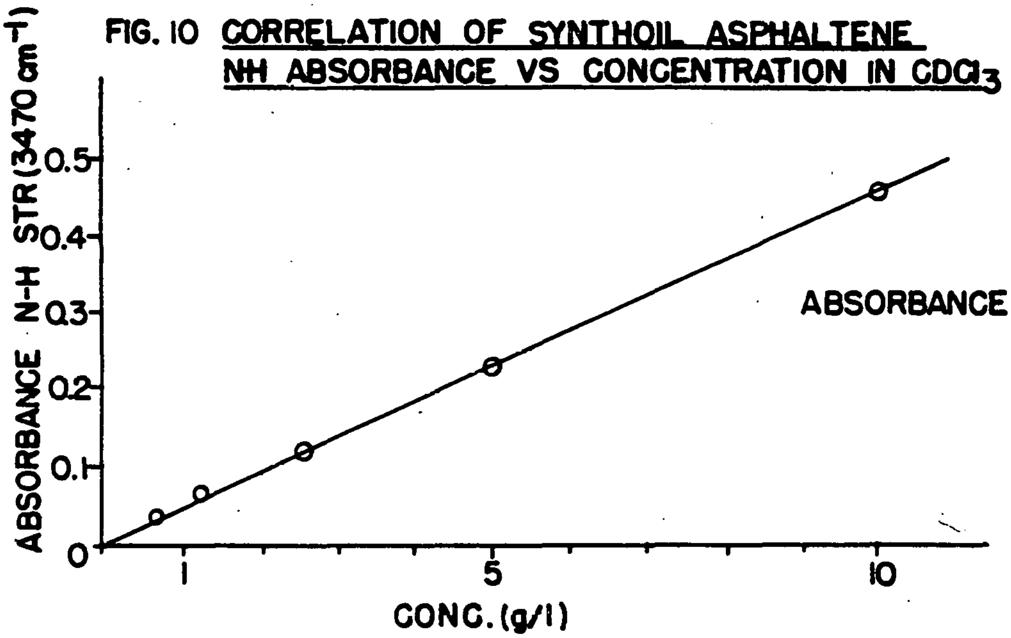

ABSORBANCE = 0.046 CONC.
L = 1 cm

FIG. 11 CORRELATION OF SYNTHOIL ASPHALTENE OH ABSORBANCE VS CONCENTRATION IN $CDCl_3$

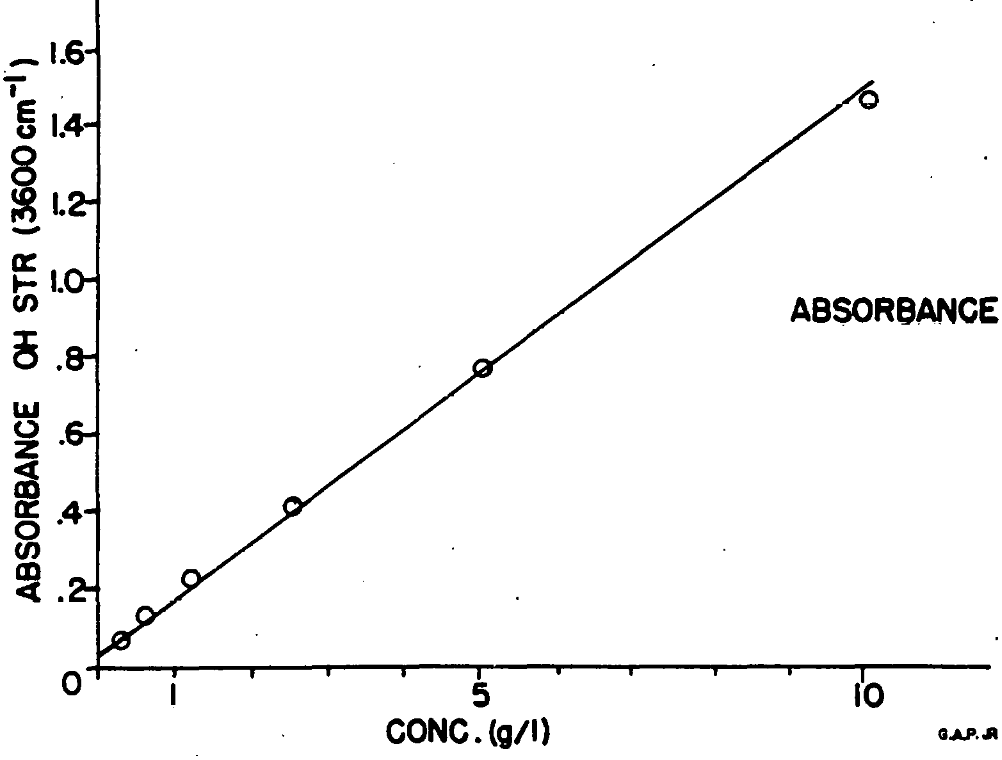

ABSORBANCE = 0.15 CONC.
L = 1cm

FIGURE 12. CORRELATION OF ASPHALTENE ABSORBTIVITY OF OH STRETCH (3600 cm^{-1}) VS. WT% OH FROM NMR ANALYSIS OF SILYLATED ASPHALTENES

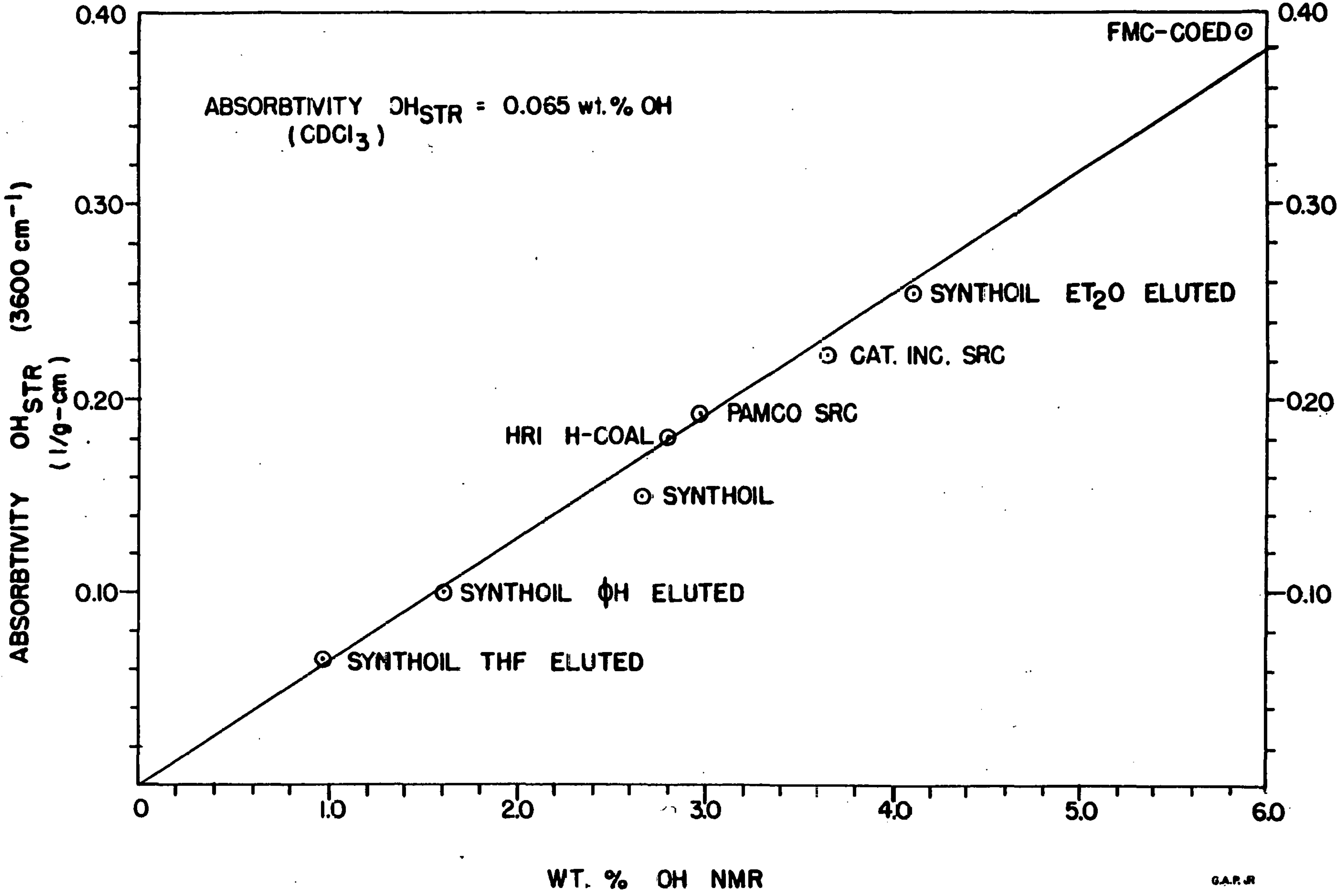

Table IV Infrared Absorptivity Values For Asphaltene OH and NH Stretches

Asphaltene	Absorptivity OH_{STR} (3600 cm^{-1}) (1/g - cm)	Absorptivity NH_{STR} (3470 cm^{-1}) (1/g - cm)
Synthoil	0.15	0.046
Synthoil Benzene Eluted	0.10	0.062
Synthoil ET_2O Eluted	0.26	0.023
Synthoil THF Eluted	0.06	0.026
HRI H-Coal	0.18	0.044
FMC-COED	0.39	0.024
PAMCO SRC	0.19	0.058
CAT, INC. SRC	0.22	0.037

between a_{NH} and weight percent pyrrolic nitrogen obtained from elemental analysis of chromatographically separated (15) or HCl treated (12) asphaltenes which were also subjected to methylation to remove remaining basic nitrogen (3) (Fig. 13). These methods for determining phenolic oxygen and pyrrolic nitrogen may be superior to methods which require the use of low molecular weight model compounds. Snyder (16) has shown that molar absorptivity values show a decrease with increasing molecular weight for carbazoles from petroleum.

These results may then be used to calculate ether oxygen and basic nitrogen by difference from total oxygen and nitrogen[a]. The results for Synthoil asphaltene and its silica gel chromatography fractions are presented in Table V . When the values for the separated asphaltene are arithmetically combined, the calculated total asphaltene values obtained are in good agreement with the values obtained experimentally for the original unseparated asphaltene. The results indicate that the benzene eluted fraction contains high proportions of OH and NH ($OH/O_{total} = 0.67$, $NH/N_{total} \cong 1$). The diethyl ether eluted fraction contains a large proportion of OH and a small fraction of NH ($OH/O_{total} = 0.76$, $NH/N_{total} = 0.20$). The THF fraction contains only small proportions of OH and NH (0.20 each). The starting unseparated asphaltene contains a majority of both OH and NH (0.69 and 0.53 respectively). The presence of phenolic and pyrrolic species in the basic fractions tends to support the idea that asphaltenes are made up of amphoteric molecules containing both acid/neutral and basic groups as well as acid/neutral, and basic molecules.

---

[a] This method was applicable to all cases except for the FMC-COED asphaltene where IR absorption bands were observed at 3400 cm^{-1} and 1650 cm^{-1} which may be assigned to the NH and C=O stretches of the amide nitrogen. In such cases a correlation would have to be developed for calculating separate amide and basic nitrogen concentrations.

FIG. 13 CORRELATION OF ASPHALTENE ABSORBTIVITY OF NH STRETCH ($3470\ cm^{-1}$) VS WT. % PYRROLIC NITROGEN

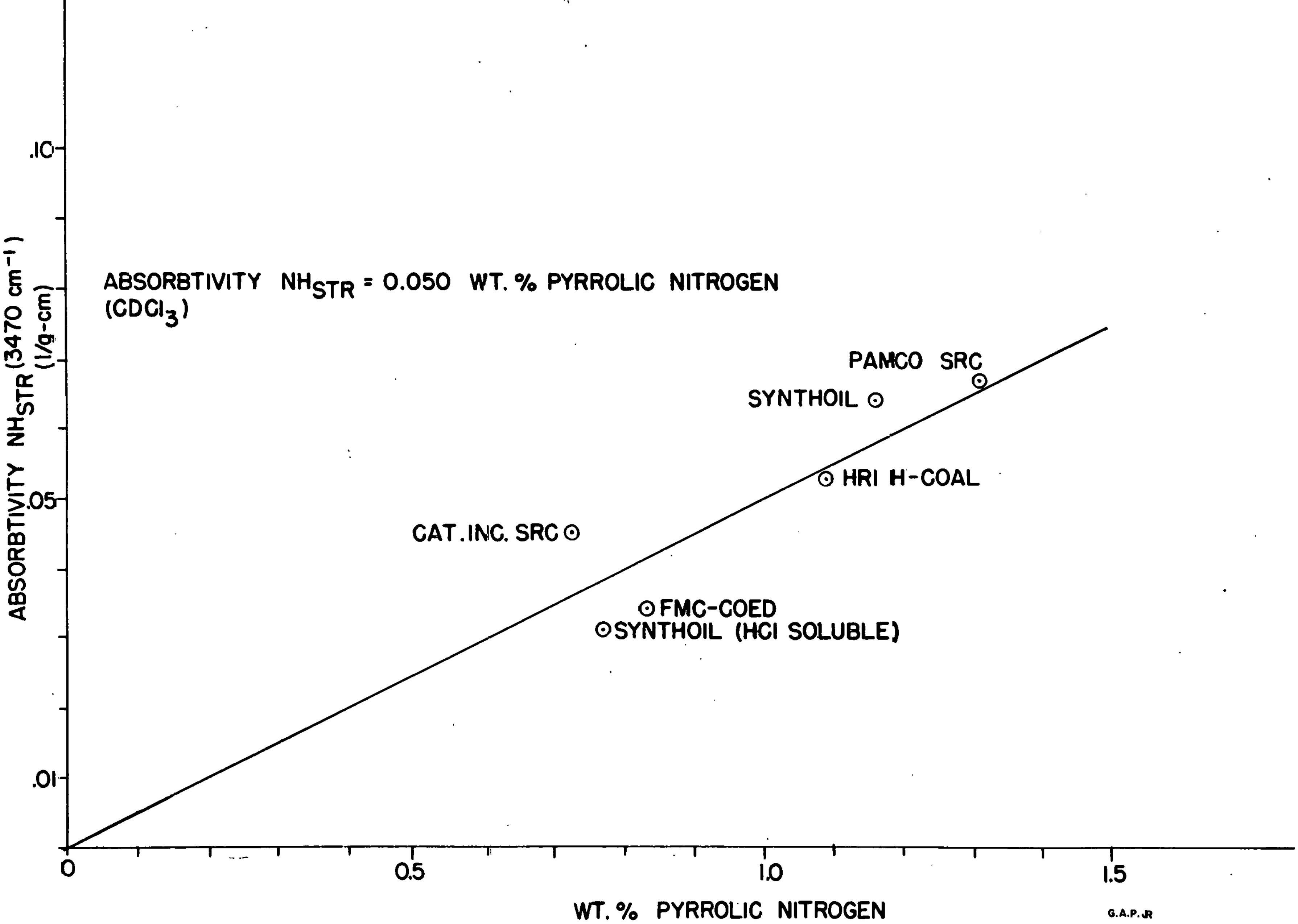

G.A.P. JR

Table V. Synthoil Asphaltene and Silica Gel Chromatography Fractions Nitrogen and Oxygen Analyses

	-------- % Oxygen -----			-------- % Nitrogen ----			% Wt.
Sample	Total[a]	Hydroxyl[b]	Ether[c]	Total[d]	Pyrrolic[e]	Basic[f]	Fraction
Benzene Eluted	2.39	1.61	0.78	1.07	1.24	(0)	45
ET_2O Eluted	5.40	4.11	1.29	2.30	0.45	1.85	37
THF Eluted	5.97	1.19	4.78	2.86	0.52	2.34	18
Original Asphaltene	3.89	2.67	1.22	1.74	0.93	0.81	100
Calculated Total Asphaltene	4.15	2.45	1.69	1.84	0.82	1.02	100

[a] By difference from ultimate analysis.

[b] From NMR analysis of trimethylsilylated asphaltene TMS area.

[c] Total Oxygen-Hydroxyl = Ether.

[d] From ultimate analysis.

[e] From IR Absorbtivity NH stretch.

[f] Total Nitrogen-Pyrrolic = Basic.

The oxygen and nitrogen analyses for asphaltenes from five demonstration processes are presented in Table VI. The results show that the OH/O_{total} values range from 0.59 to 0.83, and the pyrrolic NH/N_{total} values range from 0.53 to 0.74. The FMC-COED pyrrolic NH could not be determined unambiguously due to the presence of possible amide type NH functional groups.

(b) VPO Investigation

The VPO molecular weights of coal-derived oils and resins vs. concentration in THF have been determined and are shown in Table VII. The results show that association of oils is very small and can be neglected in THF over the concentration range of 4-30 g/l, whereas that of resin does take place. Generally, the molecular weights of oils are the lowest among the coal liquid fractions. Although the molecular weights of some oils have not been determined, they should be investigated in the next Quarter to support this conclusion. Also, the results show that the self-association of carbene is stronger than that of asphaltene, while the self-association of resin is the weakest.

The VPO molecular weights of mixtures of coal-derived resin and asphaltene vs. concentration in THF have also been determined and are shown in Table VIII. The results indicate that the association takes place for those mixtures in THF over the concentration range of 6-60 g/l. All of the mixtures afforded positive linear correlations between concentration and molecular weight except for the mixture of Synthoil, resin and asphaltene. The slopes of the linear correlation lines of PAMCO SRC mixtures decrease as the percentages of resin in the mixtures increase. Since the slope of the MW vs. concentration curve is a measure of association, it indicates that the association of the mixtures become weaker as the weight percentage of resin increases. It may be assumed that

Table VI. Asphaltene Oxygen and Nitrogen Analyses

	----- % Oxygen ------			------ % Nitrogen ----		
Asphaltene	Total[a]	Hydroxyl[b]	Ether[c]	Total[d]	Pyrrolic[e]	Basic[f]
Synthoil	3.89	2.67	1.22	1.74	0.93	0.81
HRI H-Coal	4.96	2.92	2.04	1.61	0.88	0.73
FMC-COED	7.11	5.88	1.23	1.70	(0.47)[g]	(1.23)[g]
PAMCO SRC	4.67	2.96	1.71	1.57	1.16	0.41
CAT. INC. SRC	4.58	3.65	0.93	1.25	0.73	0.52

[a] By difference from ultimate analysis.

[b] From NMR analysis of trimethylsilylated asphaltene TMS area.

[c] Total Oxygen-Hydroxyl = Ether.

[d] From ultimate analysis.

[e] From IR Absorbtivity NH stretch.

[f] Total Nitrogen-Pyrrolic = Basic.

[g] This sample showed IR absorption at 3400 cm^{-1} which may belong to amide type NH, therefore, Total Nitrogen-Pyrrolic = Basic + Amide Nitrogen.

Table VII Molecular Weight of Coal Liquid Products vs. Concentrations[a] in THF

		Least Squares Equation	Cor. Coeff.	MW at Infinite Dilution
Synthoil	Oil	$MW = 0.26 \pm 0.05c + 245 \pm 0.8$	0.87	245
	Resin	$MW = 0.86 \pm 0.30c + 252 \pm 5.1$	0.61	252
	Asphaltene[b]	$MW = 2.85 \pm 0.96c + 568 \pm 17.5$ $MW = 2.42 \pm 0.10c + 562 \pm 2.2$	0.83 0.99	567[c]
	Carbene	$MW = 5.97 \pm 0.28c + 861 \pm 6.5$	0.989	861
HRI	Oil	----	------	---
	Resin	$MW = 1.00 \pm 0.14c + 255 \pm 8.1$	0.87	255
	Asphaltene	$MW = 3.02 \pm 0.36c + 471 \pm 6.0$	0.95	502[c]
	Carbene	$MW = 16.84 \pm 5.48c + 1260 \pm 112.9$	0.74	1260
FMC-COED	Oil	$MW = 0.13 \pm 0.17c + 276 \pm 2.8$	0.24	276
	Resin	$MW = 0.50 \pm 0.14c + 298 \pm 2.5$	0.52	298
	Asphaltne	$MW = 0.56 \pm 0.10c + 382 \pm 1.9$	0.39	370[c]
	Carbene	$MW = 1.30 \pm 0.15c + 326 \pm 3.0$	0.93	326
Cat. Inc. SRC	Oil	-----	----	----
	Resin	$MW = 0.53 \pm 0.18c + 326 \pm 3.1$	0.50	326
	Asphaltene[b]	$MW = 1.11 \pm 0.38c + 486 \pm 7.6$ $MW = 2.25 \pm 0.27c + 502 \pm 4.5$	0.77 0.95	477[c]
	Carbene	$MW = 4.08 \pm 0.47c + 1228 \pm 9.1$	0.97	1228
PAMCO SRC[d]	Oil	------	----	----
	Resin	$MW = 1.22 \pm 0.39c + 320 \pm 6.1$	0.58	320
	Asphaltene	$MW = 1.8 \pm 0.16c + 502 \pm 3.3$	0.96	545[c]
	Carbene	$MW = 4.8 \pm 1.67c + 1051 \pm 38.4$	0.69	1051

---

a. Conc., g/l.
b. Results from two samples prepared independently.
c. Ave. MW at zero concentration.
d. Vacuum distillation residue.

Table VIII. Molecular Weight of Mixtures[e] of Coal-Derived Resin and Asphaltene vs. Concentration[a] in THF

		Least Squares Equation	Cor. Coeff.	MW at I.D.[b]	Theoretical MW	%Dev.[c]
PAMCO SRC[d]	Resin	$MW = 1.22 \pm 0.39c + 320 \pm 6.1$	0.58	320	--	--
	5/6Resin+1/6Asphaltene	$MW = 0.29 \pm 0.04c + 324 \pm 1.5$	0.87	324	350.0	-7.4
	2/3Resin+1/3Asphaltene	$MW = 0.33 \pm 0.19c + 362 \pm 6.7$	0.34	362	381.0	-5.0
	1/2Resin+1/2Asphaltene	$MW = 0.54 \pm 0.06c + 427 \pm 1.9$	0.91	427	411.0	+3.9
	1/3Resin+2/3Asphaltene	$MW = 0.58 \pm 0.06c + 441 \pm 2.0$	0.93	441	441.0	0.0
	Asphaltene	$MW = 1.8 \pm 0.16c + 502 \pm 3.3$	0.96	502	--	--
Synthoil	Resin	$MW = 0.86 \pm 0.30c + 252 \pm 5.1$	0.61	252	--	--
	½Resin+½Asphaltene	$MW = -1.10 \pm 0.28c + 410 \pm 9.6$	0.63	410	407	+0.7
	Asphaltene	$MW = 2.42 \pm 0.10c + 562 \pm 2.2$	0.99	562	--	--
HRI	Resin	$MW = 1.00 \pm 0.14c + 255 \pm 8.1$	0.87	255	--	--
	½Resin+½Asphaltene	$MW = 1.02 \pm 0.07c + 332 \pm 2.3$	0.95	332	363	-8.5
	Asphaltene	$MW = 3.02 \pm 0.36c + 471 \pm 6.0$	0.95	471	--	--
FMC-COED	Resin	$MW = 0.50 \pm 0.14c + 298 \pm 2.5$	0.62	298	--	--
	½Resin+½Asphaltene	$MW = 0.09 \pm 0.02c + 309 \pm 0.8$	0.68	309	340	-9.1
	Asphaltene	$MW = 0.56 \pm 0.10c + 382 \pm 1.9$	0.89	382	--	--
Cat. Inc. SRC	Resin	$MW = 0.53 \pm 0.18c + 326 \pm 3.1$	0.60	326	--	--
	½Resin+½Asphaltene	$MW = 0.22 \pm 0.19c + 466 \pm 6.9$	0.23	466	414	+12.6
	Asphaltene	$MW = 2.25 \pm 0.47c + 502 \pm 4.5$	0.95	502	--	--

---

[a] conc., g/l.

[b] I.D. means infinite dilution.

[c] %Dev.=(MW at I.D.- Theoretical MW at I.D.) /Theoretical MW at I.D.

[d] Vacuum distillation residue.

[e] Resin and asphaltene are mixed in weight percentage.

when resin is added into asphaltene solution, it tries to dissociate the self-associated asphaltene polymer to form resin-asphaltene molecules. This dissociation becomes stronger and stronger as more and more resin is added. More specifically, it means that resin-asphaltene interaction is preferred over asphaltene-asphaltene self-association. The molecular weights of all mixtures, obtained by extrapolating the plots to infinite dilution, are close to the theoretical molecular weights which are the arithmetically combined molecular weights of resin and asphaltene. This suggests that the dissociation of those mixtures tends to go to completion in THF at infinite dilution. Since the association of asphaltene in THF is not so strong as in benzene, it is hard to distinguish a small degree of dissociation in THF by adding resin to it and some results in Table VIII are not so good. In the next Quarter, the VPO molecular weights of those mixtures in benzene will be taken to study the interaction of resin and asphaltene.

(c) Particle Size Determination by Transmittance Electron Microscopy (TEM)

We previously discussed experimental procedures and results concerning our research on particle and cluster size determination of coal-derived asphaltene dimensions by TEM (17,18,19). Despite the development of computer assisted image processing techniques, it was not possible to obtain resolvable TEM pictures of isolated asphaltene molecules or clusters. It may be that individual asphaltene molecules, or even small clusters of asphaltenes, are transparent to electron microscopy due to their low densities. Therefore, two modifications of previous experiments were carried out: carboids were used instead of asphaltenes because of their larger size, and a metal shadowing technique was used to enhance resolution.

The metal shadowing technique was developed by Hall (20), and has been used mainly in studies of biomacromolecules such as DNA (20), RNA (21), and proteins (22,23,24). In our experiment, a control grid was prepared by metal shadowing a SiO film sprayed only with pyridine (glass distilled grade) (Fig. 14). The specimen grid, however, was sprayed with a small quantity of a dilute (5 mg/2500 ml) solution of Synthoil carboid in pyridine before the metal was shadowed (Fig.15). From the photographs taken at 113,000x we can see a fairly homogeneous (small grains of metal uniformly distributed) control grid, and a specimen grid that shows several distinguishable particles (indicated by dark spots due to piling up of metal on the side facing the metal source) accompanied by shadows (indicated by transparent or white spots due to the absence of metal). The fact that all shadows are in the same direction indicates that they are genuine shadows rather than artifacts on the photoplate. With a shadowing angle of 1:9, the observed shadow lengths of 90-270 Å suggest heights of 10-30 Å for

Figure 14 Control: Pyridine Deposited on SiO, then Shadowed with Platinum

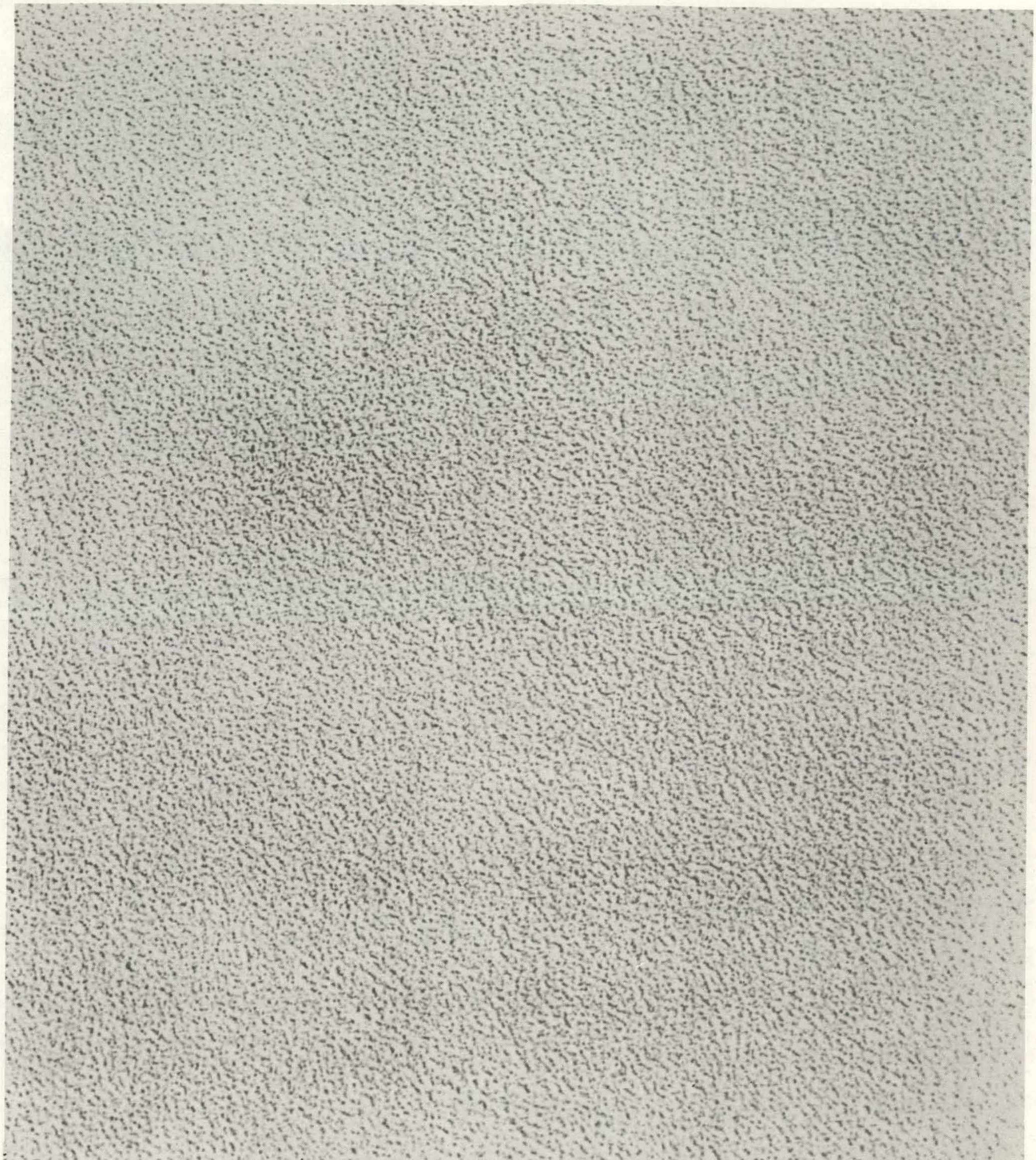

Figure 15 Specimen: Carboid Dissolved in Pyridine, Deposited on SiO, then Shadowed With Platinum vapor. (Each particle is pin-pointed by an arrow, the direction of which is that of the incoming platinum vapor. It is characterized by a dark (metal grain piling) leading edge with a white trailing shadow.

the particles. The width of the shadows is from 100 to 200 Å suggesting particle diameters of 100-200 Å (Fig. 16). Such dimensions are much larger than the dimensions of individual carboid molecules previously determined by the X-Ray-NMR method (3). Therefore, it appears that only aggregates of carboid molecules, stacked in 4-8 overlapping sheets are being observed with our present techniques. Calculations based on the weight of carboid sprayed onto a given area of surface, and the average MW of Synthoil carboid (1000), indicate that the upper limit of distinguishable molecules is ≈ 0.2 wt.% of the total present. The rest are too small to cast any noticeable shadow. In other words, 99.8% of the carboid deposit may have sizes smaller than the above described average TEM observable carboid clusters.

To improve the resolution of the technique, less metal should be deposited to give smaller grains in the background. Some bigger reference object of known size may also be introduced to give a more exact calibration. Such an object may also be used as something to focus on during photograph taking. These improvements may allow us to observe species of smaller size, and individual carboid molecules.

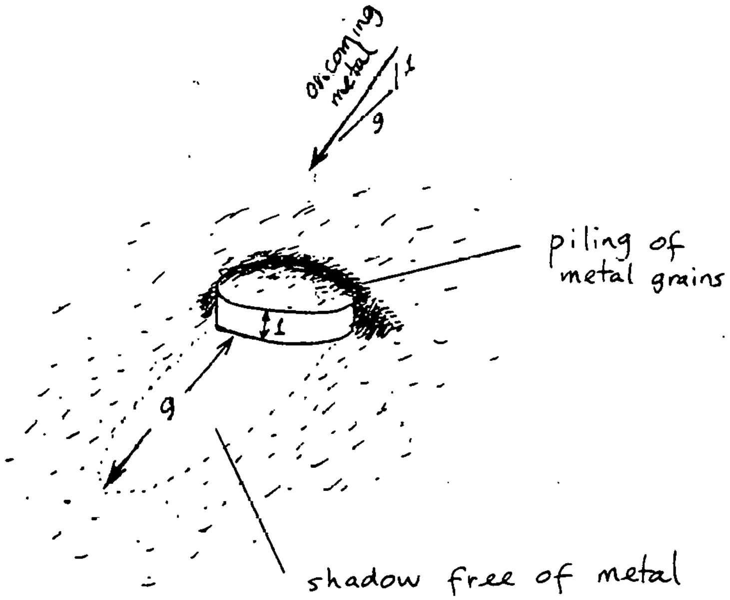

Figure 16. The Metal Shadowing Technique for EM.

(d). Densimetric Methods of Structural Analysis

Densimetric methods of structural analysis have been widely used for determining the average structural character of molecules in a complex mixture. Using refractive index, density, and elementary analysis van Krevelen and co-workers developed methods for studying the structure of coal (25). In previous Quarterly Reports we presented helium density and refractive index values for various asphaltenes (14,3). We also evaluated the n-d-M method, and calculated compactness, F/Ca, values for asphaltenes (3). During the present Quarter we determined the refractive indices of all the coal liquid fractions by the extrapolation method in the solvent pyridine (Table IX). We also determined the helium densities of some of the coal liquid fractions (Table X).

Molar refraction is generally useful in aiding in structural determination. The Lorenz-Lorentz formula may be used to express molar refraction:

$$R_M = \frac{(n^2-1)\ M}{(n^2+2)\ d}$$

n= refractive index
M= MW
d= density

The molar refraction of saturated organic compounds is usually accurately given by the sum of atomic interactions ($R'_M = \sum a_i r_i$, where a_i is the number of atoms of type i in the molecule and r_i are the corresponding atomic refractions). For unsaturated molecules increments due to double bonds are included. However, for compounds having conjugated double bonds an extra increment has to be added. This increment generally rises with increasing degree of condensation for aromatic compounds. R_m is always greater than R'_M and the difference between the two is known as the molar refractometric increment I_M: $I_M = R_M - R'_M$

The refractometric increment has been shown theoretically and experimentally to be a function of the number of carbon atoms in the aromatic cluster

Table IX. Refractive Indices (n_{25}) of Coal Liquid Products[a]

Solvent Fraction	Synthoil	HRI	CAT. INC.	PAMCO	FMC -COED
Oil	1.55	1.59	1.66	1.55	1.56
Resin	1.61	1.61	1.70	1.77	1.62
Asphaltene	1.62	1.67	1.73	1.73	1.63
Carbene	1.74	1.78	1.88	1.86	1.68
Carboid	1.76	1.78	1.77	1.88	1.71

---

[a] Extrapolated to 100% in pyridine solution.

Cau (26). Even when R_M cannot be caluculated as in cases such as coal, because the molecular weight is not known, it is still possible to obtain the size of aromatic clusters by plotting I_M/C_A vs. the aromatic surface area, S ,:

$$\frac{I_M}{C_A} = f(1/S)$$

and relating S to C_{Au} (Fig.17) (26). We have calculated I_M/C_A values by use of M, d, n, elemental analyses, and fa values. We then utilized these values in conjunction with Schuyer and Van Krevelen's curve (Fig.17) to determine average aromatic cluster sizes. The preliminary results for C_{Au}, shown in Table X for the asphaltenes and the Synthoil carbene, appear generally to be too low. Only the Synthoil asphaltene, C_{Au} = 14, and the Synthoil carbene, C_{Au} = 18, values agree with the more reasonable values previously determined by the X-Ray - NMR procedure (3). It appears that either our experimental data is not accurate enough, or that the Schuyer and Van Krevelen refractometric structural parameter method is not generally applicable to coal liquid products. More work is planned in this area in the next Quarter.

When refractive indices are plotted vs. the Brown-Ladner parameters fa, (ratio of aromatic carbons to total carbons) or H_{ARU}/C_{AR} (ratio of substitutable edge atoms to total aromatic atoms) rough correlations are observed (Figs.18 ,19). Such correlations could be used as a simple means of obtaining fa, or H_{ARU}/C_{AR} values from index of refraction measurements.

FIG. 17 MOLAR INCREMENT PER GRAM ATOM AROMATIC CARBON VS AROMATIC SURFACE AREA AND CARBON ATOMS PER AROMATIC CLUSTER

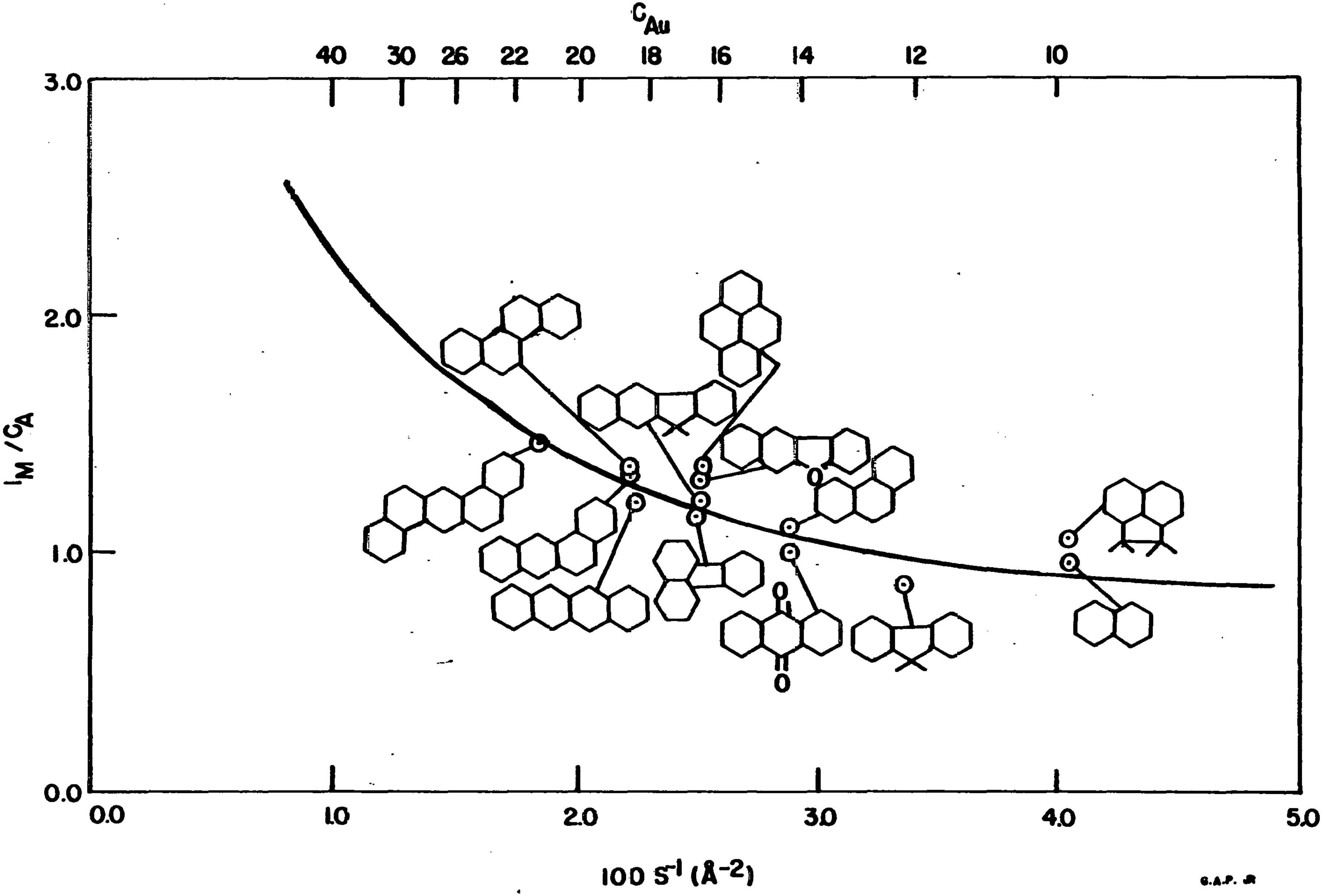

G.A.P. JR

Table X Aromatic Carbons Per Structural Unit, C_{Au}, By Molar Refraction Method[a]

Sample	M^{b}	d^{c}	n^{d}	R_M	R'_M	I_M	f_a	I_M/C_A	C_{Au}
Synthoil Asphaltene	561	1.18	1.67^{d}	177.7	145.6	32.1	0.71	1.11	14
HRI H-Coal Asphaltene	492	1.27	1.70^{d}	149.7	125.1	24.6	0.78	0.88	10
FMC-COED Asphaltene	375	1.24	1.63^{e}	107.7	96.9	10.8	0.67	0.63	$\ll 10$
PAMCO SRC Asphaltene	563	1.32	1.73^{d}	170.1	144.5	25.6	0.76	0.83	< 10
Cat-Inc SRC Asphaltene	483	1.23	1.70^{d}	151.8	125.8	26	0.80	0.89	10
Synthoil Carbene	861	1.23	1.74^{e}	282.5	222.7	59.8	0.75	1.28	18

---

a. Schuyer and van Krevelen, Ref. 26

b. VPO infinite dilution value in THF.
c. Helium displacement method.
d. Average value extrapolated to 100% solute concentration in solvents benzene, THF, and DMF.
e. Extrapolated to 100% solute concentration in solvent pyridine.

FIG. 18 REFRACTIVE INDEX VS. AROMATICITY FOR COAL LIQUID PRODUCTS

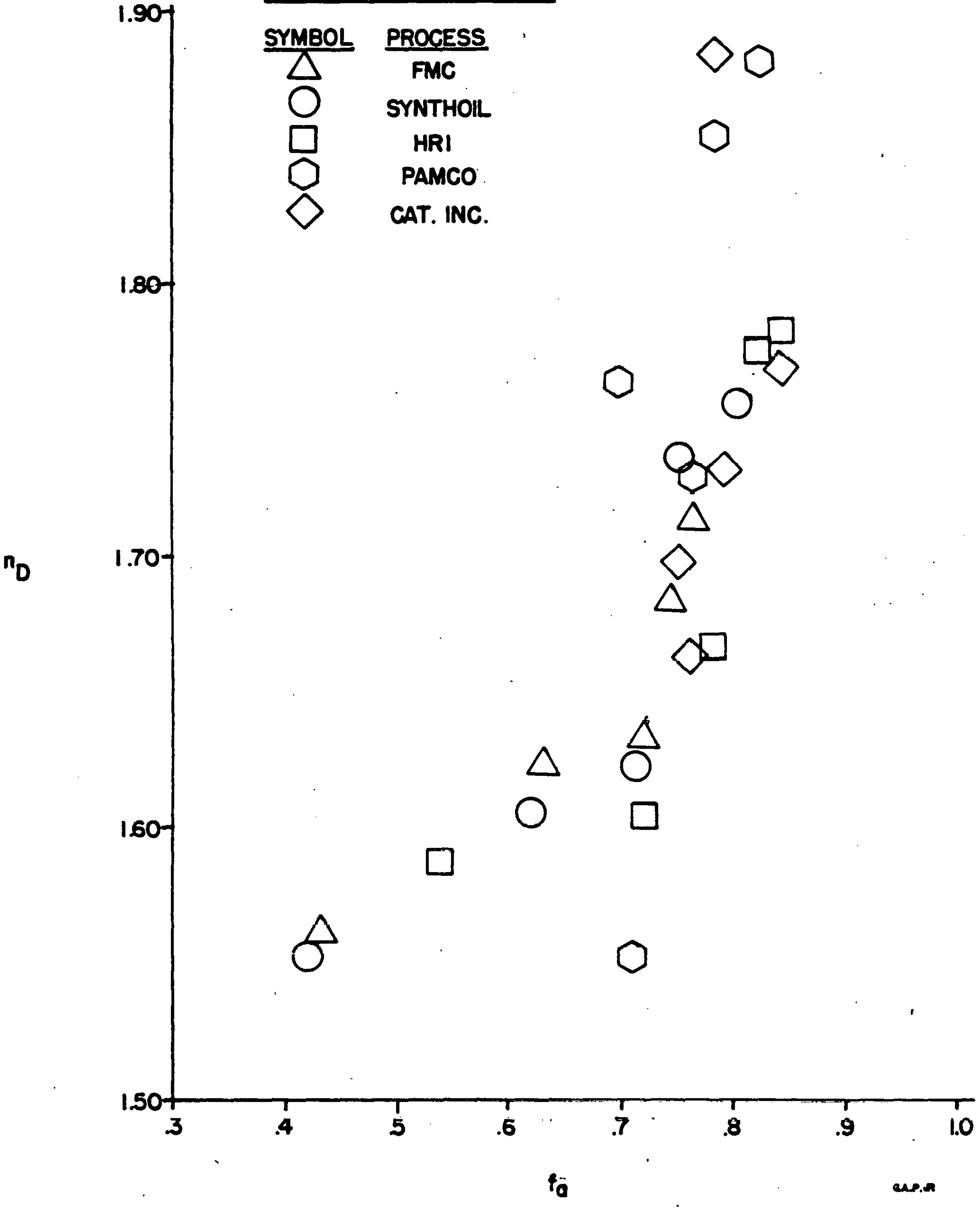

FIG. 19 REFRACTIVE INDEX VS. H_{ARU}/C_{AR} FOR COAL LIQUID PRODUCTS

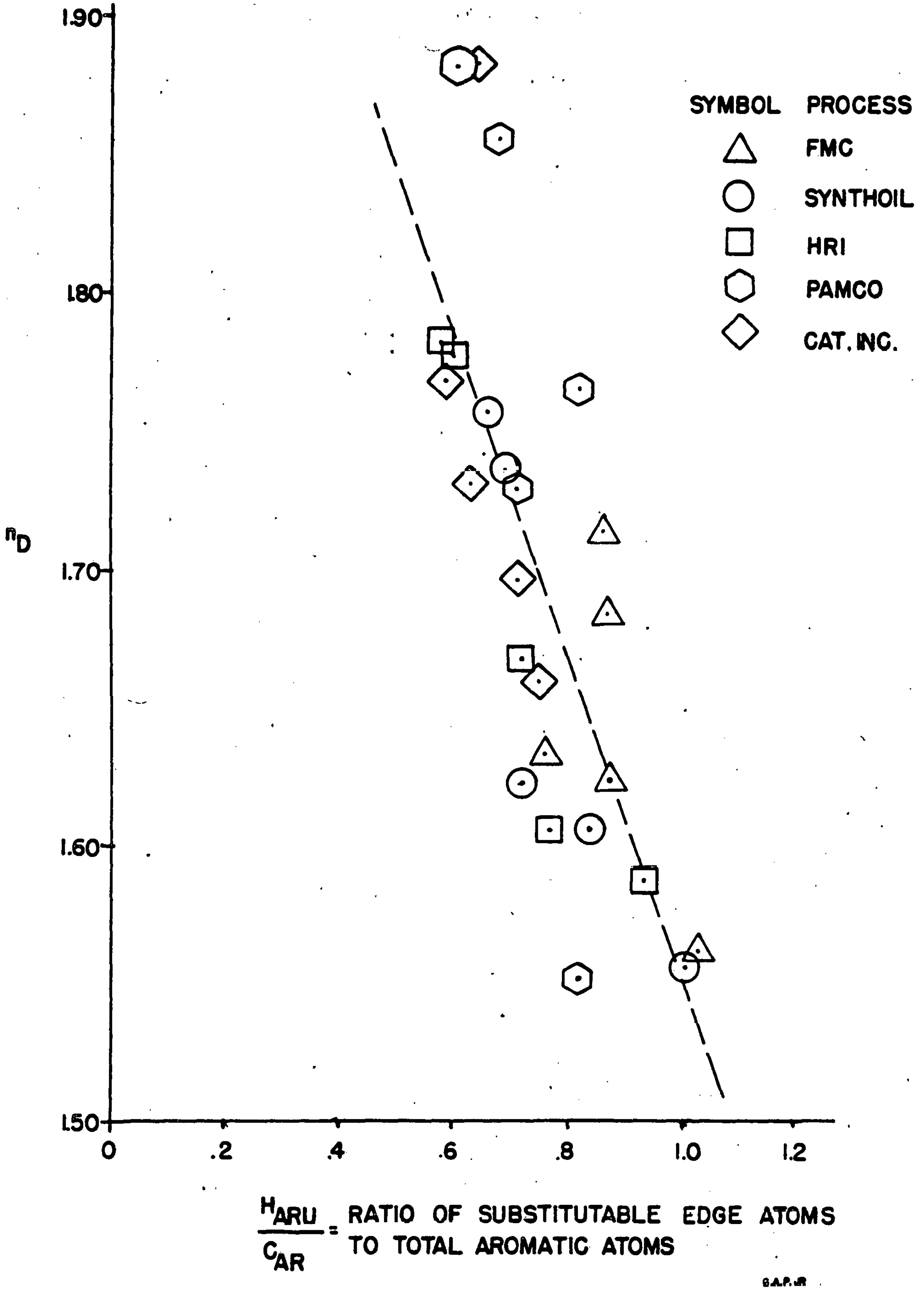

Conclusion

Preparative scale GPC separation of Synthoil asphaltene was carried out on styrene-divinyl benzene packing (Bio-Beads S-X 8). The elution took place in the order of high to low molecular weight. The C/H ratio generally increases as the MW decreases. The aromaticity, f_a, shows a steady increase from 0.58 to 0.76 with fraction number, while the number of carbon atoms per saturated substituent, n, decrease from 2.5 to 1.5. The fraction of available aromatic edge atoms occupied by substituents, also decreases from 0.69 to 0.37 as the elution volume increases. These results can be interpreted in terms of aromatic ring systems, with large saturated substituents eluting first. As the elution volume increases the saturated substituents decrease in number and size resulting in the molecules becoming smaller and more aromatic. The size of the average aromatic ring system, as measured by the ratio of substitutable aromatic edge atoms to total aromatic atoms, H_{aru}/C_{ar}, appears to go through a minimum.

Thermal treatment of a Synthoil coal liquid solvent fraction (oil + resin) in tetralin (1:2 wt. ratio) at 232°C for 20 hours resulted in the transformation of 3 - 10 % of the oil + resin into asphaltene. These results support the proposed reversibility of coal liquefaction steps:

$$\text{Asphaltene} \rightleftharpoons \text{Oil} + \text{Resin}$$

Pyrolysis of coal-derived asphaltenes has been shown to produce residues that are characteristic of coalesced mesophase. Asphaltenes from three liquefaction processes, Catalytic Incorporated SRC, Synthoil, and FMC-COED, were pyrolyzed under a nitrogen atmosphere to 420°C. The samples were heated at 20°C/hr. to 360°C and at 5°C/hr. to 420°C. Crossed polarized light reflection micrographs were obtained for each of the pyrolyzed samples. Phenolic oxygen is believed to cause cross-linking and reduce mesophase plasticity. The Synthoil asphaltene has the lowest phenolic oxygen content, 2.71 % , and forms a mesophase that remains plastic at 420°C giving the coarse, deformed structure. The Catalytic Inc. SRC asphaltene contains slightly more phenolic oxygen, 3.38 % , and forms a coarse but not a deformed structure. And the FMC-COED contain 5.90 % phenolic oxygen and forms the fine isotropic structure which results from crosslinking and solidification at a temperature below 420°C.

Infrared measurements were carried out with a large path cell (1 cm) in order to measure absorbance as a function of concentration in dilute solution down to 0.3 g/1 where association between asphaltenes is not significant. Plots of absorbance vs. concentration were generally linear below concentrations of 10 g/1 and could be extrapolated to a value of zero at infinite dilution. The extrapolated slopes of the linear portion of such plots were used to obtain absorptivity values. These values for a_{OH} afforded a good linear correlation vs. weight percent OH, determined by the silylation method, a_{OH} = 0.065 wt. % OH , and a fair correlation between a_{NH} and weight percent pyrrolic nitrogen obtained from elemental analysis of chromatographically separated or HCl treated asphaltenes which were also subjected to methylation to remove remaining basic nitrogen, a_N = 0.050 wt. % Pyrrolic Nitrogen. These methods for determining phenolic oxygen and pyrrolic nitrogen may be superior to methods which require the use of low molecular weight model compounds. Snyder has shown that molar absorptivity values show a decrease with increasing molecular weight for carbazoles from petroleum. Ether oxygen and basic nitrogen may then be calculated by difference from total oxygen and nitrogen.

VPO molecular weight studies indicate that coal-derived oils and resins undergo very little association in the solvent THF in the range 4 - 30 g/l. The molecular weights of resin-asphaltene mixtures, at infinite dilution, are close to the theoretical molecular weights obtained by arithmetically combining molecular weight, and weight fractions of resin and asphaltene. This indicates that dissociation of such mixtures tends to go to completion in THF at infinite dilution.

References

1. DOE (ERDA) Report No. FE-2031-10, Dec. 1977.
2. DOE (ERDA) Report No. FE-2031-3, Mar. 1976.
3. DOE (ERDA) Report No. FE-2031-12, June 1978.
4. D. D. Lawson and J. D. Ingham, Nature, 223, 614(1969).
5. I. Schwager and T. F. Yen, Fuel, 57, 100(1978).
6. FMC Corp., Char Oil Energy Development, Report No. 56, Interim Report No.1, Office of Coal Research, U. S. Dept. of the Interior, 1970.
7. DOE (ERDA) Report No. FE/496-149, June 1978.
8. P. L. Walker, W. Spackman, P. H. Given, E. W. White, A. Davis, and R. G. Jenkins, Ann. Rep. Penn. State Univ. to EPRI, Res. Proj. 366-1, Dec. 1975.
9. J. E. Zimmer, J. L. White, Mol. Cryst. Liq. Cryst., 38, 177(1977).
10. J. D. Brooks and G. H. Taylor, Chemistry and Physics of Carbon, 4, 243 (1968).
11. Petroleum Derived Carbons , Am. Chem. Sec. Symposium Series, 21, 282 (1976).
12. H. N. Sternberg, R. Raymond, and F. R. Schweighardt, Science, 188, 49 (1975).
13. I. Schwager, W. C. Lee and T. F. Yen, Anal. Chem., 49, 2363 (1977).
14. DOE (ERDA) Report No. FE-203-11, Mar. 1978.
15. I. Schwager and T. F. Yen, in Liquid Fuels from Coal, (R. T. Ellington, Ed.) Academic Press, N. Y., 1977.
16. L. R. Snyder, Anal. Chem., 41, 314 (1969).
17. DOE (ERDA) Report No. FE-2031-6, Dec. 1976.
18. DOE (ERDA) Report No. FE-2031-7, Mar. 1977.
19. DOE (ERDA) Report No. FE-2031-8, June 1977.
20. C. E. Hall, Ann. of N.Y. Acad. of Sci., 81, 723 (1959).
21. C. E. Hall and Bills, Virology, 17, 123 (1962).
22. C. E. Hall et al., J. Biophys. Biochm. Cytol., 6, 407 (1959).

23. H. S. Slayter and C. E. Hall, J. Mol. Biol., 8, 593 (1964).

24. A. J. Rowe and R. J. Weitzman, Ibid, 13, 345 (1969).

25. D. W. Van Krevelen, Coal, Elsevier, N. Y., 1961.

26. J. Schuyer and D. W. Van Krevelen, Fuel, 33, 176 (1954).

☆U.S. GOVERNMENT PRINTING OFFICE:1979-640-092/ 648